



# The Interaction Between Twin Tunnels Beneath a Sandy Slope-2D Numerical Study

Ashraf K. Nazir<sup>1</sup> · Ahmed Nasr<sup>1</sup> · Asmaa Saeed<sup>1</sup>

Received: 2 January 2024 / Accepted: 20 July 2024  
© The Author(s), under exclusive licence to Indian Geotechnical Society 2024

**Abstract** Most of previous numerical studies on twin tunnels were simplified by assuming perfectly horizontal ground surfaces above the tunnels and a 50% stress release ratio ( $\lambda_d$ ). Moreover, often studies focused on deformations at the slope's ground surface, neglecting lining forces in the first tunnel caused by the second tunnel excavation under asymmetric surrounding soil pressure. A 2D finite element model is established to address this gap and provide a case study for practical engineering applications involving geotechnical problems with stress release. This paper analyzes twin tunnels under a sandy slope using the PLAXIS 2D program by the convergence–confinement method. The study highlights the influence of releasing stress rate of the second tunnel on the displacement in the first tunnel lining and slope surface and its role in selecting the most appropriate relative position and spacing distance between two tunnels. The results revealed that the displacements in the slope surface caused by the second tunnel may increase or decrease with the variation in spacing values depending on the position of the new tunnel. Also, the impact of various parameters on the behavior of the slope and the first tunnel after constructing a new tunnel, including tunnels configuration, soil properties, slope angle, tunnel cover depth, and construction sequence, is examined. By optimizing these parameters, different charts have been suggested to help

designers and control surface settlement caused by twin tunnels. Also, understanding these issues can help the designers and practitioners make informed decisions during new tunnel construction.

**Keywords** Numerical modeling · Tunnel cover depth · Spacing and rotation · Stress release coefficient · Sandy slope

## Abbreviations

$C$	Depth from slope mid-point to the tunnel crown
$D$	Diameter of the tunnel
$H_{max}$	Maximum horizontal displacement
$k$	Bending moment coefficient in the lining
$M_I$	Bending moment in the first tunnel lining after excavating the new one
$M_O$	Bending moment in the first tunnel lining before excavating the new one
$N_I$	Axial force in the first tunnel lining after excavating the new one
$N_O$	Axial force in the first tunnel lining before excavating the new one
$S$	Spacing between the tunnels center line
$S_{max}$	Maximum surface settlement
$\alpha$	Slope angle
$\beta$	Axial force coefficient in the lining
$\gamma$	Soil unit weight
$\theta$	Rotation angle of the new tunnel
$\lambda_d$	Stress release coefficient

✉ Asmaa Saeed  
asmaa133224@f-eng.tanta.edu.eg

Ashraf K. Nazir  
Ashraf.Nazir@f-eng.tanta.edu.eg

Ahmed Nasr  
ahmed.nasr@f-eng.tanta.edu.eg

<sup>1</sup> Structural Engineering Department, Faculty of Engineering, Tanta University, Tanta, Egypt

## Introduction

In general, the construction of tunnels at shallow and deep depths can meet the increased demand for transportation. In

these cases, predicting the impact of new tunnel construction on an existing one is critical for the optimal design. New tunnel construction changes the stress and deformation in the ground, which could ultimately affect the serviceability of a nearby tunnel. The tunnels in urban areas are not located generally in great depths in the soil. Therefore, the effects of the tunneling process activities can easily reach the surface. The searches on the interaction of twin tunnels can be divided into four categories: field observation, centrifuge model testing, analytical empirical methods, and finite element approaches (Peck 1969 [1]; Herzog 1985 [2]; Addenbrooke and Potts 2001 [3]; Kim et al. 2001 [4]; Koungelis and Augarde 2004 [5]; Karakus et al. 2007 [6]; Hage and Shahrour, 2008 [7]; Chakeri et al. 2015 [8]). In the case of horizontal ground at the surface, many researchers have used 2D and 3D numerical modeling for twin tunnel interaction analysis, with a focus on ground deformations. Ng et al. (2004) [9] investigated the interactions and the lagging distance between parallel twin tunnels constructed using the NATM method in soft clay using three-dimensional numerical simulations. The location of the maximum settlement value offsets to the centerline of the pillar width until the lagging distance equals 2.5 times the tunnel diameter. Hage and Shahrour (2008) [7] carried out a 2D numerical modeling and observed that the construction procedure, the spacing between tunnels, and the new tunnels' relative position controlled the profile and magnitude of the settlement and bending moment. They proposed that the magnitude of the settlement and the structural forces in the first lining are maximum when the spacing is minimum and after spacing  $S=3D$ , there is no significant effect. Karademir (2010) [10] performed a parametric study on three-dimensional modeling of twin parallel NATM tunnels in sand considering the advancement of the second tunnel on the existing one. Li et al. (2013) [11] performed a series of 3D numerical simulations of the interaction between two shield tunnels by FLAC3D in layered soil. The distribution and magnitude of soil pressure, deformations, and internal forces induced in the existing tunnel after the excavation of a new shield tunnel were affected significantly by both the alignment and the spacing between the two tunnels. Abdelrehim et al. (2018) [12] carried out a parametric study to suggest a minimum practical and safe spacing distance between the driven new tunnels and the existing ones without the need for the relatively expensive soil strengthening techniques. Islam and Iskander (2022) [13] studied numerically the ground deformations above twin tunnels using three cover-to-diameter ( $C/D$ ) ratios, three possible construction sequences, five angular relative positions, and five angular spacing. Pedro et al. (2022) [14] performed a parametric study on two-dimensional modeling of twin parallel tunnels. They confirmed that the stiffness of the linings and the initial stress

conditions affect significantly the magnitude of the lining forces and the interaction effects.

In the context of shallow tunnels parallel to the slope, shallow tunnels are common at mountainsides, at tunnel entrances, and in valleys. Slopes can be dangerous for tunnel construction as the slopes may themselves be unstable and could cause tunnel failure. Most previous studies on tunnels constructed in sloping ground which investigates the stability represent case studies in reality. Du and Huang (2008) [15] examined the effect of different excavation sequences for twin tunnels in weak rock under unsymmetrical pressure by numerical simulation and model test. Lei et al. (2015) [16] performed a model test of shallow buried tunnels under unsymmetrical loading and found that as the bias angle increases, the difference of surrounding rock pressure between the shallow and deep side of tunnel increases. In addition, with the advance of excavation, the stress release rates and deformation increase until the tensile stress on the ground surface on the deep side appears, thereby producing fractures on the superficial ground. Das et al. (2017) [17] examined the stability of twin tunnels in jointed rock for asymmetric parallel and concluded that the crown was less stable than the invert of the tunnel. Vlachopoulos et al. (2018) [18] provided better insight into the influence of twin tunnels passing through a slope within Weak Rock Masses at a shallow overburden. They revealed that after the tunneling process, the factor of safety decreased and the potential shear failure surface was relocated by passing through the tunnels. Zhang et al. (2019) [19] studied the mechanism of a single tunnel excavation's influence on slope stability. To address the geological circumstances of the landslide on the slope where the tunnel is located, it is recommended to stabilize the slope prior to tunnel construction. They disclosed that the range of 1.5–2.5 times the tunnel diameter is the impact of the region of excavation of tunnels on slope deformation.

Regarding the searches on the supporting structure, Banerjee and Chakraborty (2018) [20] presented charts for designing circular tunnels with specific stability and calculating liner pressure for achieving stability in sloping ground in cohesive-frictional soils by the lower bound finite element limit analysis. The primary support failure mechanism was discussed by Yang et al. (2020) [21] using field observations, monitoring, and 3D numerical simulation of a shallow and asymmetrically loaded tunnel entrance. They recommended that secondary lining should be applied after tunnel excavation and cutting slope can decrease the load in damage cases. Song et al. (2021) [22] found that the supporting structure reduces the total displacement, stress, and strain of the tunnel and the slope surface, and the deformation of the rock slope is significantly correlated with the distance from the slope surface. Also, they studied the impact of the excavation of twin tunnels on the mechanical characteristics and deformation of laminated slopes.

In other words, asymmetric surrounding rock pressure acts on the tunnel support system, generating asymmetric deformation and increasing the risk of cracks and other risks such as collapse and damaged linings [23]. For this reason, earlier studies focused on tunnel strengthening in real case studies. Qiu, et al. (2022) [23] performed a 3D numerical simulation on the behavior of fluid–solid coupling in shallow buried tunnels under different biased terrain. Their models identified and analyzed the places where the biggest displacement, stress, water pressure, and water input occur during the tunnel excavation process. Based on numerical and field data, Li et al. (2023) [24] investigated the surface settlement and stability of the slope at the portal for shallow twin tunnels. They investigated the best order for excavation and suggested strengthening the tunnel’s inverted arch support in the badly weathered rock layer. The majority of those studies focused on the stability and deformations recorded at the slope’s ground surface. Limited studies were carried out to study surrounding soil pressure and internal force distribution of supporting structures under terrain conditions. As it is evident in this review, the complicated problem of the construction of a new tunnel on the first tunnel beneath a sloping ground considering various parameters, has not been addressed in the literature. The evaluation of the lining forces in the first tunnel caused by the second excavation is frequently ignored or viewed as a minor issue under asymmetric surrounding soil pressure and needs further investigation. To address this gap in the state of the art, a 2D finite element model has been established focusing on both deformations and lining forces. The primary aim of this research is to illustrate the influence of the new tunnel construction on the first tunnel beneath a sandy slope considering tunnels configuration, soil properties, slope angle, tunnels cover depth, construction sequence, and the stress release ratio. Also, the study illustrates the role of the stress release ratio in the selection of the most appropriate relative position and spacing distance between two tunnels. Therefore, the following section presents background on the stress release ratio. In addition, the research strategy for FEM modeling steps and the analysis approach are illustrated in Fig. 1.

### Background on Stress Release Ratio:

Loss of confinement in the underground context often includes other construction work such as deep excavation, cut-and-cover technique, and shield tunneling. The actual practice of 2D FEM is widely popular and demanded, given constraints of costs and technology in analysis. However, 2D plane-strain models require an assumption for the deconfinement process. The concept of stress releasing ratio was introduced to utilize 2D FEM to simulate 3D stress state, thereby representing the 3D constraint effect. The stress release ratio is crucial for understanding soil strength, which is derived

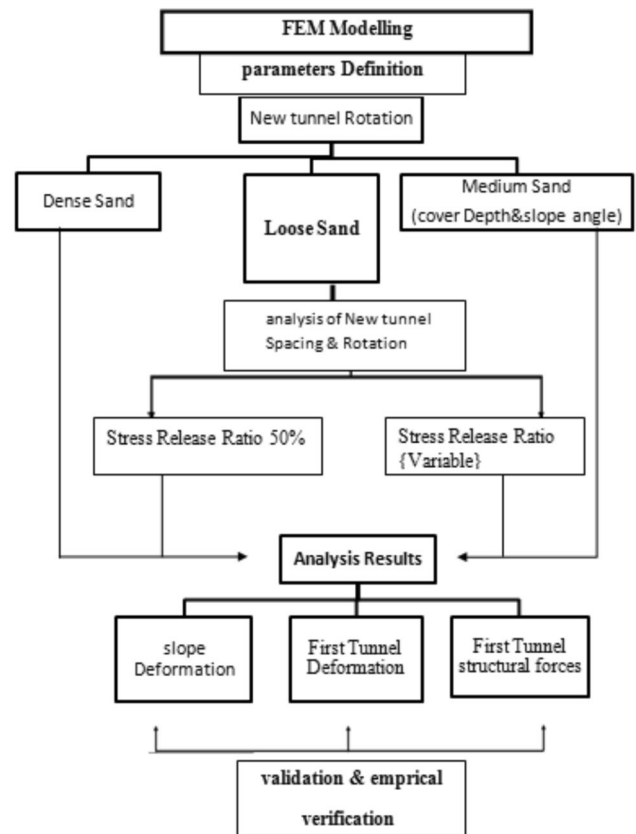


Fig. 1 Flowchart of the work

from confinement in underground construction. Regarding tunnel design approaches, the partial stress release factor, which closes the gap between the excavated boundary and the lining, was changed to take workmanship quality and tunneling aspects into account (Dias et al.2014) [25]. The deconfinement method allows for the pre-displacement of the soil near the tunnel boundary to be taken into consideration before the structural element is installed. The equivalent approaches that are available to control the deconfinement process are the convergence–confinement method (CCM), the gap method, the volume loss control method, and the contraction method. Because the convergence–confinement technique (CCM) is the basis of this work, a brief overview of the CCM will be included. The theoretical framework established by Panet and Guenot (1982) [26] can be used to calculate the progress of excavation and installation of delayed supports in the ground around a tunnel by applying a stress release coefficient ( $\lambda_d$ ). The idea is that the initial stresses ( $\sigma_\rho$ ) around the tunnel are applied in two steps. In the first step, the stresses ( $\sigma_r$ ) are applied to the unsupported tunnel. The radial displacement of the tunnel wall begins, and the internal pressure  $\sigma_r$  progressively decreases until it satisfies the specified stress relaxation ratio ( $\lambda_d$ ). Equation (1) is used to get the value of ( $\sigma_r$ ). This signifies that

the lining is not yet in place and that the surrounding soil can deform. The whole relaxation ( $\lambda_d=1$ ) is applied in the second stage, and the remaining load is distributed over the lining and the soil.

$$\sigma_r = \sigma_0(1 - \lambda_d) \quad (1)$$

where  $\lambda_d$  is a dimensionless coefficient that represents the stress relaxation in the tunnel walls at various excavation stages and  $\sigma_0$  is the initial stress of the soil.

Macroscopic stress release during excavation is the displacement release of the surrounding soil. Stress release and displacement release are time–space effect problems caused by tunnel excavation. Because stress release is closely associated with ground displacements, estimating the ground displacements might lead to a stress release evaluation. Many researchers investigated the relationship between tunnel liner pressure and radial deformation (Fenner 1938 [27], Pacher 1964 [28]). It is found that high pressures will act on the support structure if it is installed too soon. Increasing the liner time for installation means a large stress release rate and induces the loosening mechanism, which causes a shear failure in the surrounding soil. Many factors influence the value of the stress release coefficient ( $\lambda_d$ ), including tunnel excavation length to diameter, tunnel depth, soil properties, tunnel shape, lining stiffness, and time effects (Negro and Eisenstein (1997) [29], and Mousivand et al. 2017 [30]). It is very difficult to predict the effect of all these factors on stress release ratio. For this reason, the stress release ratio should be defined using in situ measurements collected throughout the tunneling process (Mroueh and Shahrour 2008 [31] and Do 2014 [32]). However, many researchers proposed using tables and diagrams to quickly estimate the stress reduction factor ( $\lambda_d$ ) (Negro and Eisenstein (1997) [29]). Muir Wood (1975) [33] proposed a 50% stress reduction for lining design. However, some researchers proposed a range of stress release coefficients ( $\lambda_d$ ) from 0.3 to 0.5 (Kim 2006 [34], Svoboda and Mašín 2009 [35]). In other words, different stress reduction factors, according to Moller and Vermeer (2008) [36], must be utilized to generate good estimations of surface settlement and normal forces. They study suggested that a single  $\lambda_d$ -value is insufficient for reproducing lining forces and displacements in 3D calculations, suggesting stress-releasing values ranging from 0.6 to 0.7 for surface settlement and 0.3 for lining forces.

In the context of the role of stress release ratio in construction works, Zhang et al. (2008) [37] studied the impact of stress-releasing ratio and boundary scope on 2D FEM simulations of open excavation. They examined the relationship between stress releasing ratio and excavation width or depth using 3D simulation models, providing a reference for practical analysis. Scholars also investigated by numerical simulations the influence of a variation of the stress release

factor ( $\lambda_d$ ) of a single tunnel on surface settlement and lining forces (Mroueh and Shahrour 2008 [31], Do (2014) [32] and Heidarzadeh et al. (2020) [38]). Moreover, the tunnel face stability was studied numerically by investigating the stress release on the tunnel face by Li et al. (2014) [39]. In other words, researchers found that the stress relief process affects tunnel seismic response based on applied strain magnitude, increasing until the critical strain is reached, then reduced [40]. Earlier researchers have studied the relationship between stress release ratio and displacement release rate by model tests, field monitoring, and numerical simulations to explore appropriate excavation methods based on stress release considerations (Nie et al. (2024) [41]). In the context of the destabilization level of the slope, The numerical study of Causse et al.(2015) [42] reveals that increasing deconfinement before a structure's implementation leads to stronger slope destabilization, causes a reduction of stress (axial forces, shear forces and moments). The effect of the stress release ratio was also not thoroughly analyzed in case of tunneling beneath sloping ground surface. Despite there being very few attempts on the influence of deconfinement ( $\lambda_d$ ) in the case of a single tunnel beneath an inclined surface, no attempts to demonstrate how the stress release ratio affects twin tunnel and slope performance under asymmetric pressure. In addition, it was not considered how this factor may be considered in the selection of the most appropriate relative position and spacing distance between two tunnels. This work presents a case study for practical engineering applications involving geotechnical problems with stress release effects related to relative position and spacing distance between two tunnels. Furthermore, in the case of an inclined surface, this work provides some additional guidance on possible interaction effects between twin tunnels for parallel and piggyback designs. As a result, the research findings can be used to develop an analytical approach for similar engineering constructions.

## Materials and Methods

A series of 2D numerical analyses of single and twin tunnels was carried out under a sandy slope (3:1) using PLAXIS 2D program [43] by applying the convergence–confinement method. The first tunnel is excavated in loose sand below the middle of the inclined ground surface with an angle  $\alpha = 18^\circ$  at a depth  $C_1 = 2D$  (reference case). The slope is located in the middle of the model. A new tunnel will be constructed parallel to the first one, horizontally and vertically, using the TBM method. Three parallel multiple tunneling geometries are investigated here (Fig. 2a). Tunnel axes are horizontally aligned at ( $\theta = 0^\circ$  and  $180^\circ$ ) and vertically aligned at ( $\theta = -90^\circ$ ). The parametric study includes varying the spacing,

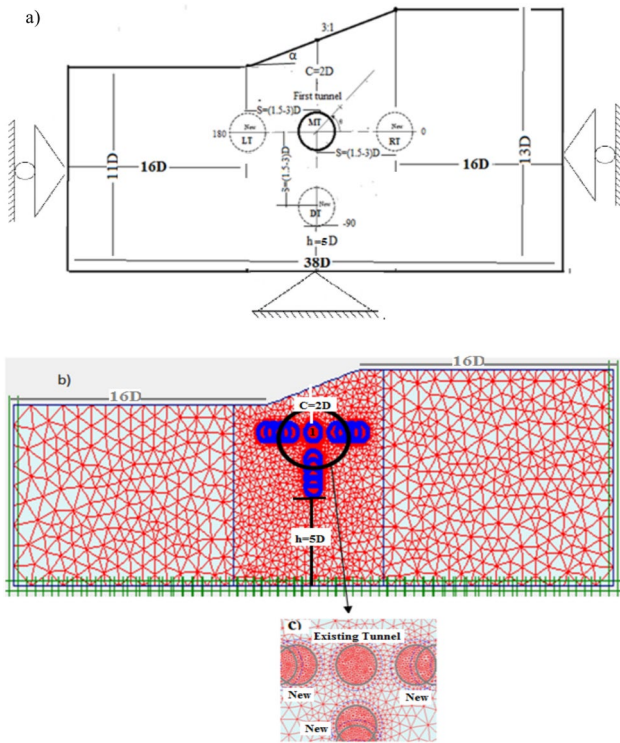


**Fig. 2** a Layout of the geometry; b finite element mesh with boundary conditions for  $C_1/D=2$ ,  $S/D$  varies from 1.5 to 3, and c) zoomed view of refined mesh around the tunnel

depth of burial, relative locations, slope angle, excavation sequences, and stress release coefficient, as shown in Table 1. All tunnels are assumed to be identical with the same diameter ( $D$ ) of 5 m and stress relaxation ratio ( $\lambda_d$ ). The construction stages of the tunnels are performed by PLAXIS 2D, as follows:

1. Phase (0): gravity loading is generated as the initial phase depending on the soil self-weight.

2. Phase (1): deactivating the soil cluster. A stress relaxation ratio ( $\lambda_d$ ) is applied to the tunnel wall which is defined in terms of  $\sum M$ stages in PLAXIS program.
3. Phase (2): installing the tunnel support by activating the lining on the tunnel boundary ( $\lambda_d = 1.0$ )

Phases two and three will be repeated for the second tunnel using the same stress release coefficient. First, the deconfinement rate induces by the tunnel excavation and waiting before tunnel lining implementation vary according to different factors as discussed in the literature, however the deconfinement rate of the tunnel face was recommended approximately of 50% by Muir Wood (1975) [33]. A value of  $\lambda_1 = \lambda_2 = 0.5$ , in line with the suggestion of Hage and Shahrour, 2008 [7], was adopted in all analyses. Also, to highlight the deconfinement rate influence, different stress release factor values of the second tunnel ( $\lambda_2$ ) considering tunnel configurations are adopted. The sand properties are listed in Table 2. Mohr–Coulomb model is employed with drained analysis to simulate the sand soil behavior. The MC model is a first-order linear-elastic-perfectly plastic model that expresses stress–strain behavior, thus no hardening or softening happens. The absence of hardening or softening input soil data in the three selected sand soil types from the literature prompted the use of the MC model. The Mohr–Coulomb model was applied to all soil types in comparative research, allowing the fundamental concept of the MC model analysis to be compared based on the soil input parameters. The soil properties were chosen for the sand slope consistent with [McGrath et al. (1999, 2002) [44, 45], Balkaya et al. (2013) [46], and Zhou et al. (2018) [47]. The tunnel lining is modeled as a linear-elastic model. Table 3 illustrates the properties of the lining. The groundwater level is considered below the surface of models; it means that dry environmental conditions are considered for the soil mass.

Numerous numerical models were created, each time with smaller mesh sizes until the changes in displacement

**Table 1** Parametric study

Scope	Parameters					
	$S$	$\alpha$ ( $^\circ$ )	$\theta$ ( $^\circ$ )	$C_1/D$	$\lambda$	Sand type
Effect of spacing ( $s$ )	1.5D, 2D, 2.5D, 3D	18	0, 180, -90	2	0.5	Loose
Effect of rotation ( $\theta$ )	2D	18	0, 180, -90	2	0.5	Loose, medium and dense
Effect of slope angle ( $\alpha$ )	2D	0, 18, 33.7	0, 180, -90	2	0.5	Medium
Effect of first tunnel depth ( $C_1$ )	2D	33.7	0	1, 2, 3, 4, 5	0.5	Medium
Effect of excavation sequence	2D	18	0, 180, -90	2	0.5	Loose
Effect of stress release coefficient ( $\lambda$ )	1.5D, 2D, 2.5D, 3D	18	0, 180, -90	2	0.1, 0.2, 0.3, 0.4, 0.5, 0.7	Loose

**Table 2** Material properties of sand soils used in this study [42–45]

Material type	Modulus of elasticity( $E$ ) kPa	unit weight( $\gamma$ ) kN/m <sup>3</sup>	Friction angle $\phi$ ( $^\circ$ )	Dilation angle $\psi$ ( $^\circ$ )	Poisson's ratio( $\nu$ )
Loose sand	$2 \times 10^4$	18	$28^0$	$5^0$	0.3
Medium sand	$4 \times 10^4$	20	$35^0$	$20^0$	0.3
Dense sand	$8 \times 10^4$	21	$40^0$	$25^0$	0.3

**Table 3** Material properties of tunnel lining used in this study (Hage and Shahrou (2008) [7])

Material behavior	Modulus of elasticity( $E$ ) mPa	Concrete unit weight( $\gamma$ ) kN/m <sup>3</sup>	Equivalent thickness( $d$ ) m	Poisson's ratio( $\nu$ )
Elastic	35,000	25	0.5	0.2

became small enough by adjusting the mesh dimensions. Furthermore, near the tunnel, the density of triangular elements is increased to improve computation accuracy. The model has dimensions similar to that of Hage and Shahrou (2008) [7]. The distinction is that the ground surface in this investigation has a shallow slope of 3:1. The boundary effect was eliminated after numerous attempts with a horizontal extension of 16D from the tunnel centerline and a vertical extent of 5D below the invert of the lower tunnel. To mimic the plane-strain model, a very fine mesh type is produced using 6-node elements. The finite element model with 20,635 nodes and 9372 elements is shown in Fig. 2b. Figure 2c shows the refined mesh around the tunnel. Bottom-line boundary conditions limit displacements in both directions; whereas, lateral boundaries impose zero horizontal displacements.

## Analysis and Results

This section discusses the results of surface deformation of the slope and the effect of new tunneling on the first parallel tunnel, with a focus on internal forces and tunnel deformations. In solid mechanics, a positive bending moment is defined as the lining of a tunnel under tension. Otherwise, it's negative. This work applies the opposite rule to axial forces. Positive vertical deformation in Plaxis means heave and negative tends to settlement toward down. Negative horizontal deformation tends to be left toward the slope downward and otherwise, it's positive.

Given the purpose of this investigation a value of  $\lambda_1 = \lambda_2 = 0.5$ , in line with the suggestion of most studies in the literature, is adopted in all analyses. The new tunnel has three relative positions: on the right side of the first tunnel ( $\theta = 0^\circ$ ), on the left side of the first tunnel ( $\theta = 180^\circ$ ), and below the first tunnel's invert ( $\theta = -90^\circ$ ). The addition of a new tunnel near the first one is predicted to affect ground deformations, lining deformation, and structural forces in the first tunnel lining. The displacements in the first tunnel lining and slope surface are caused only by the driving of the new tunnel. The maximum bending moment induced in the first lining ( $M_1$ ), represented by the moment coefficient ( $K$ ) (Hefny et al. (2004) [48] and Vinod et al. (2019) [49]), and the maximum axial force induced in the first lining ( $N_1$ ), represented by the axial coefficient ( $\beta$ ) (Kim, S.H (1996) [50]). They are expressed in Eqs. 2 and 3, respectively, as follows:

$$k = \frac{4M}{\gamma CD^2} \quad (2)$$

$$\beta = \frac{2N}{\gamma CD} \quad (3)$$

### Influence of Spacing and the position of the second tunnel:

#### The surface settlements

The settlement troughs above the first and second tunnels in loose sand are shown in Fig.3 for various spacing distances ( $S=1.5D, 2D, 2.5D$ , and  $3D$ ) and  $\lambda_1 = \lambda_2 = 0.5$ . The settlement trough over a single tunnel constructed first (in the middle of the slope) is also shown for comparison purposes. It can be noticed that the settlement trough above the twin tunnels depends on the distance between tunnels and the relative position of the new tunnel. At the same stress release ratio, as the spacing between the two tunnels increases, the settlement value over the second tunnel increases. This outcome is valid for ( $\theta = 0^\circ$ ), as shown in Fig. 3a. The reason for this is that the increase in the horizontal spacing leads the shear bands to move near the slip circle of the slope resulting in significant settlements, as shown in fig.4c. As the spacing increases, the settlement trough becomes wider toward the top zone. In contrast, as the spacing of the new tunnel increases, the surface settlement trough above the second tunnel decreases. This outcome is valid for ( $\theta = 180^\circ$ ), as shown in Fig. 3b. In the case of ( $\theta = -90^\circ$ ), It appears that the maximum settlement is not affected significantly by the variation of spacing. However, the set-

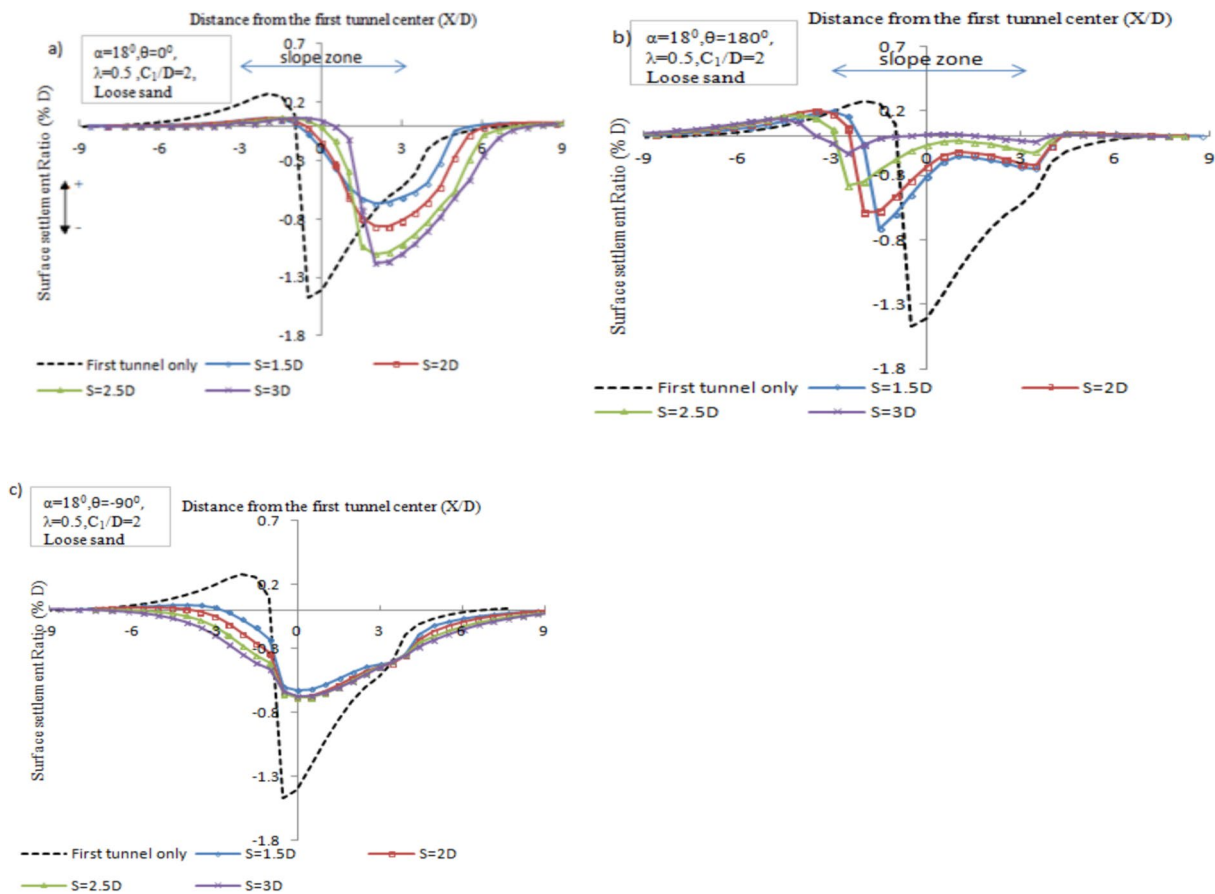


**Fig. 3** Settlement troughs above the second tunnel for  $\lambda_1=\lambda_2=0.5$  at various spacing  $S$  in different three positions of the second one: **a** ( $\theta=0^\circ$ ), **b** ( $\theta=180^\circ$ ), **c** ( $\theta=-90^\circ$ )

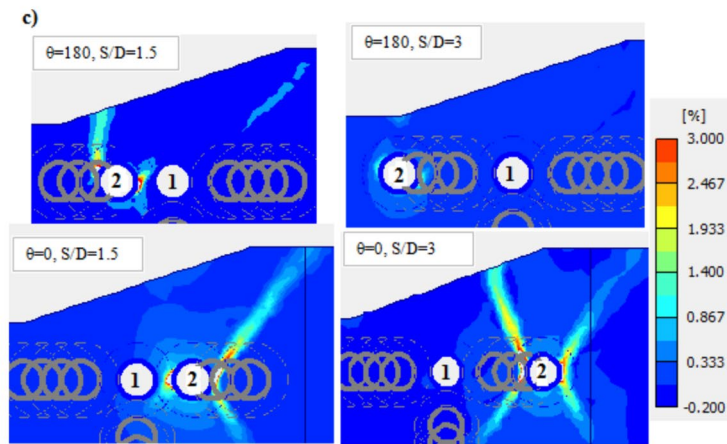
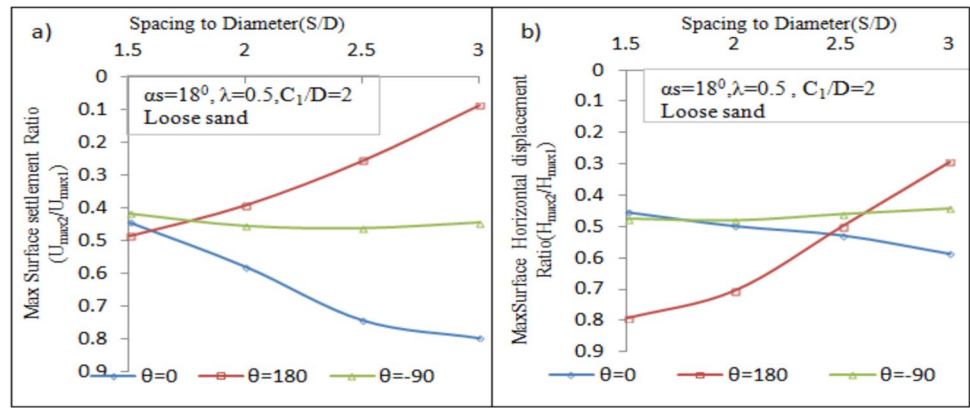
tlement trough over the second tunnel becomes wider as the spacing increases, as shown in Fig. 3c. To summarize the numerical data, two design charts have been created and are shown in Fig. 4. Both charts show (a) the maximum surface settlement for a second tunnel compared to the maximum settlement above a Greenfield (first) tunnel, and (b) the maximum horizontal displacement of the slope for a second tunnel compared to the maximum horizontal displacement for a Greenfield tunnel. These values are shown in the two charts as a function of spacing  $S$ . According to the design charts, the displacements in the slope surface caused by the second tunnel may increase or decrease depending on the position of the new tunnel. If the highest horizontal or vertical deformation of the slope surface above the first tunnel is detected, the surface displacements above the second tunnel can be simply estimated from the charts in Fig. 4a and b. Small spacing values at ( $\theta=180^\circ$ ) induce higher surface horizontal movement than the other positions. In contrast, the position of ( $\theta=0^\circ$ ) induces higher surface settlement, especially for large spacing values. Finally, at the same

$\lambda_d=0.5$  for both tunnels constructed in loose sand beneath the surface of a shallow slope (3:1), in comparison with the three relative positions of the new tunnel, the maximum value of surface settlement occurs only above the first tunnel. Moreover, constructing a new tunnel under the slope induces surface settlements higher than the surface horizontal displacement of the slope. This outcome is valid for all spacing values in different positions.

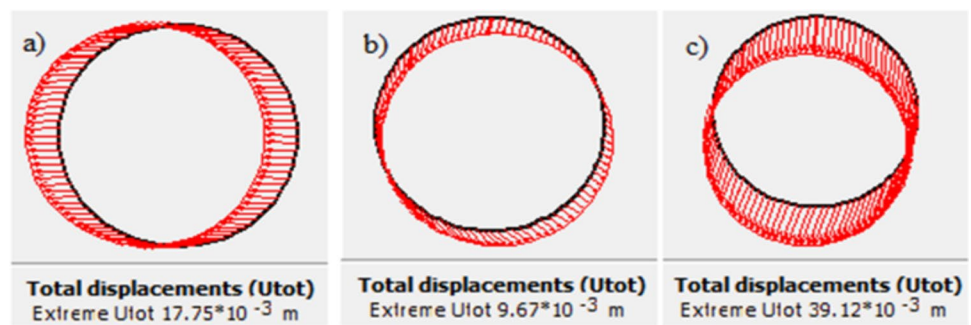
*Deformations in the First Tunnel Lining:*

Figure 5 reveals the influence of the relative position of a new tunnel on the deformation of the first tunnel. The distortion referred to the first created by driving the new tunnel. When the new tunnel is aligned at  $\theta=-90^\circ$ , the maximum deformation of the first tunnel is induced. At  $\theta=0^\circ$ , the horizontal distortion is more evident than at the other positions. However, the vertical displacement at  $\theta=-90^\circ$  has a larger impact than the other cases. The various displacement images also indicate that the impact

**Fig. 4** Effect of spacing between twin tunnels at  $\lambda_1 = \lambda_2 = 0.5$  on the surface deformations **a** maximum surface settlement ratio and **b** maximum surface horizontal movements ratio and **c** shear strain(%)



**Fig. 5** Variation of Deformation ( $m$ ) in the first tunnel for spacing ( $S = 1.5D$ ) by excavating the new one at different positions: **a** horizontally aligned at ( $\theta = 0^\circ$ ), **b** horizontally aligned at ( $\theta = 180^\circ$ ) and **c** below the invert of the first one ( $\theta = -90^\circ$ )



of the new tunnel excavation on the first lining is proportionate to the new tunnel's position on the slope. The new tunnel excavation in various positions has greater adverse effects on the first tunnel deformation in a series of: The new tunnel is vertically beneath the first ( $\theta = -90^\circ$ ) (see Fig. 5c), the new tunnel beside the first one at position  $\theta = 0^\circ$ , and the new tunnel is aligned horizontally at position of  $\theta = 180^\circ$ . The Crown Point moves horizontally in all cases toward the slope downhill due to the high interaction with the slope.

*The Straining Action in the First Lining:*

Figures.6 and 7 show the structural forces in the first tunnel resulting from the excavation of a new tunnel at different relative positions. Compared to the single case, for the new tunnel is excavated horizontally parallel to the first tunnel at the position of  $\theta = 0^\circ$  and  $180^\circ$ , the bending moment and the axial force of the first tunnel experience an increase. This increase at the position of  $\theta = 0^\circ$  is larger than that induced at  $\theta = 180^\circ$ . It may be because the first tunnel in the case of  $\theta = 0^\circ$ , carries a larger portion of load from the second one



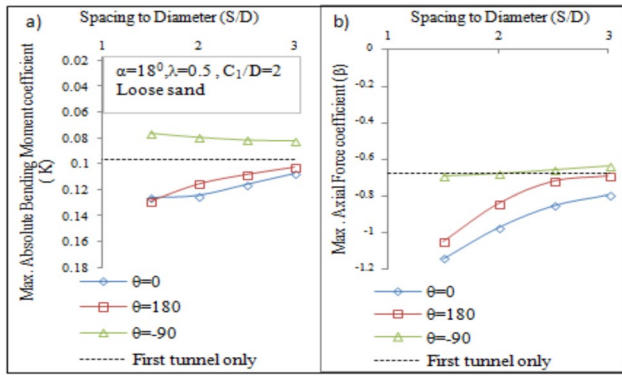
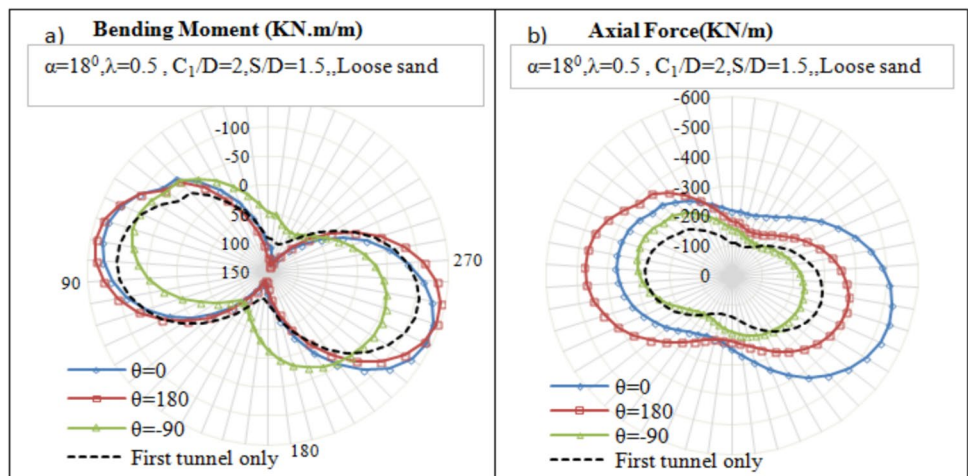


**Fig. 6** Effect of spacing between twin tunnels at  $\lambda_1=\lambda_2=0.5$  on the straining actions of the first tunnel: (a) bending moment coefficient ( $k = \frac{4M}{\gamma CD^2}$ ) and b axial force coefficient ( $\beta = \frac{2N}{\gamma CD}$ ).

which is loaded with high overburden stress. Moreover, the movement of soil surrounding the new tunnel toward the soil between the two tunnels resulting in more pressure on the first one (Do 2014) [32]. In contrast, at the position of  $\theta = -90^\circ$ , the structural forces experience a decrease in the first tunnel lining compared to the single case. However, some of the internal forces in the first tunnel lining have been changed in sign from positive to negative and vice versa, as shown in fig.7. Thus, all critical sections should be checked related to the new straining action. These results agree with the study of (El-Naiem et al. 2007) [51]. At the position of  $\theta = -90^\circ$ , negligible effect on the maximum bending moment and maximum axial force coefficient in the first tunnel by changing the spacing  $S$  between the two tunnels. Finally, the moment coefficient and the axial force coefficient of the first tunnel will increase significantly after excavating the new one at spacing less than (2.5-3) times the tunnel

**Fig. 7** Variation of bending moment (kN m) and axial force (kN/m) in the first tunnel for  $\lambda_1=\lambda_2=0.5$  and spacing ( $S=1.5D$ ) in different three positions of the new tunnel



diameter. This outcome is valid for all three positions of the new tunnel.

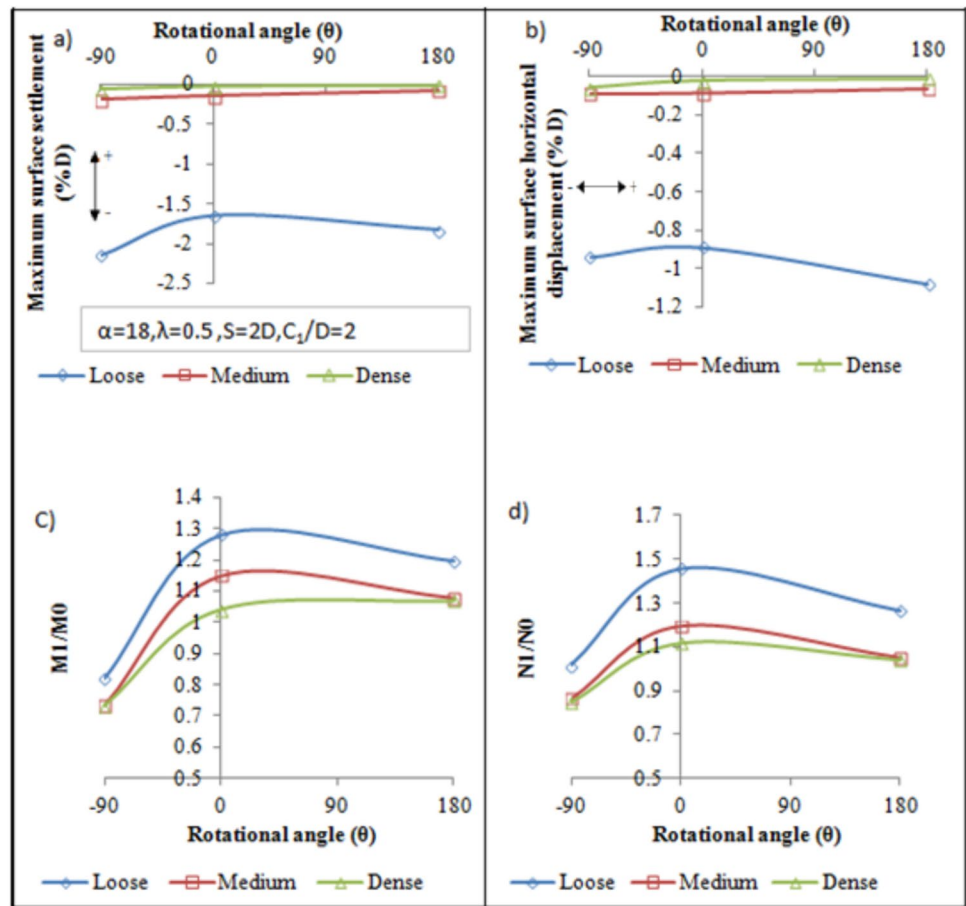
**The Influence of the Soil Type:**

As expected in all the different scenarios, it can be observed in Fig. 8 that as the relative density of the sandy slope increases, for a constant slope angle( $18^\circ$ ) and constant spacing ( $S=2D$ ), the surface settlement and the horizontal displacement decrease, meaning that the stability of the slope improves as well. Furthermore, the results differed significantly between loose and medium soils compared to medium and dense sand soils. Therefore, the loose sandy slopes should be compacted if it is possible before excavating the tunnels. For medium and dense sand soils, the position of  $\theta = -90^\circ$  induces the highest maximum surface settlements and horizontal movements in the slope. Despite the position of  $\theta = -90^\circ$  inducing maximum surface settlements in the case of loose sand soil, the maximum surface horizontal displacement occurs at the position of  $\theta = 180^\circ$ . The maximum structural forces in the first tunnel occur in loose sand and at the position of  $\theta=0^\circ$ . The maximum bending moment and the axial force in the first tunnel are higher by about 22% and 32%, respectively, than that induced in the case of the first tunnel only.

**Influence of Different Stress Release Factor Values of the Second Tunnel ( $\lambda_2$ ):**

As mentioned before, it can use the stress release coefficient to express the time of installation lining. In this section, different values of ( $\lambda_d$ ) ranging from 0.1 to 0.7 will be selected for the two tunnels constructed in loose sand at different spacing and positions of the new tunnel. The whole stress release process ( $\lambda_d=1.0$ ) is not used because

**Fig. 8** Effect of soil type on a the surface settlement, b the surface horizontal movement, c the moment ratio, and d the axial force ratio



the computation cannot achieve an equilibrium condition. Furthermore, substantial soil deformation will occur, which is similarly unrealistic for shallow tunnels constructed in loose soil. The following data demonstrate the effect of the new tunnel at various lining installation intervals by varying the stress release coefficient ( $\lambda_2$ ) on the surface settlement and the first lining deformation considering ( $\lambda_1 = \lambda_2$ ).

*Surface Settlements*

Three design charts have been prepared to summarize the numerical observations, as presented in Fig. 9. The maximum surface settlement referred to that induced by the driving of the new tunnel only. Both charts provide (a) the maximum slope settlement ratio at the position of  $\theta = 0^\circ$ , (b) the maximum slope settlement ratio at the position of  $\theta = 180^\circ$ , and (c) the maximum slope settlement ratio at the position of  $\theta = -90^\circ$ . All charts provide these data as a function of the stress release ratio of the second tunnel ( $\lambda_2$ ). According to the design charts, the surface settlement caused by the second tunnel is dependent on the installation period of the second tunnel lining. It is clear that after releasing a specific amount of stress, the displacements induced in the slope surface vary substantially with the stress release coefficient

( $\lambda_2$ ) in a nonlinear relationship. As the stress release ratio ( $\lambda_2$ ) increases, the maximum surface settlement above the second tunnel increases sharply, especially after  $\lambda_2 = 0.6$  at a position of  $\theta = 180^\circ$  in Fig. 11b.

According to slope stabilization, after a certain percent of releasing stress ( $\lambda_2$ ), the slope displacement exceeds the allowable limit ( $1^\circ\text{mm}$ ). As a result, the installation time of the new tunnel lining can control the slope-strengthening process. For spacing ( $S = 1.5D$ ) as an example, the critical design values of the stress release ratio of the new tunnel ( $\lambda_2$ ) are 30% for  $\theta = 0^\circ$  and  $-90^\circ$ . Whereas, it reaches 40% at the position of  $\theta = 180^\circ$ . After these values, the slope will require strengthening.

*The first Tunnel Lining Displacement:*

Taking the smallest spacing distance ( $S = 1.5D$ ) as a worst case for the first lining due to the high interaction between the two tunnels. The deformation referred to hereafter is deformation induced in the first one by the driving of the new tunnel only. Figure 10 illustrates that the stress release value of the new tunnel ( $\lambda_2$ ) can control the movements of the first lining. By increasing the value of  $\lambda$  from 0.3 to 0.7, the vertical displacement of all lining points changed

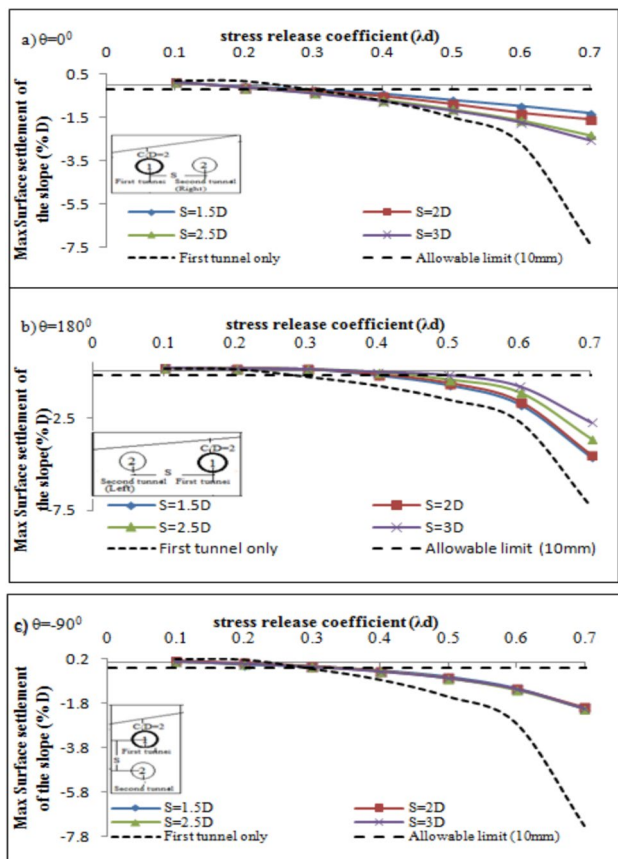


**Fig. 9** Effect of different values of the stress coefficient of the second tunnel ( $\lambda_2$ ) constructed in loose sand at different spacing  $S$  and positions on the maximum surface settlements ( $m$ ) **a** at the right side of the first one ( $\theta=0^\circ$ ), **b** at the left side of the first one ( $\theta=180^\circ$ ) and **c** below the invert of the first one ( $\theta=-90^\circ$ )

from up heave to settlement for all positions of the new tunnel. The results also determined the critical design values of  $\lambda_2$  and the critical zones in the lining that need strengthening (close to the new tunnel). At the position of  $\theta=0^\circ$ , the critical value of  $\lambda_2=0.65$ , and the zone from crown to right needs strengthening first (Fig. 10a). After the value of  $\lambda_2=0.5$  in case the position of  $\theta=180$ , the zone from crown to left requires strengthening first (Fig. 10b). Otherwise, at the position of  $\theta=-90$ , the right parts of the tunnel from crown to invert should be strengthened if the value of ( $\lambda_2$ ) exceeds 0.3 (Fig. 10c). This means that in the latter case, the new tunnel lining must be installed at early stages to reduce the cost of strengthening.

**Influence of the Construction Order (Sequence):**

The optimal excavation sequence of twin tunnels will be explored for spacing  $S=2D$  between the two tunnels. The first tunnel is excavated below the middle of the inclined ground ( $\alpha=18^\circ$ ) at depth of  $c_1=2D$  (reference case, as

mentioned in Fig. 2a. Three cases of excavation sequences are conducted, as follows:

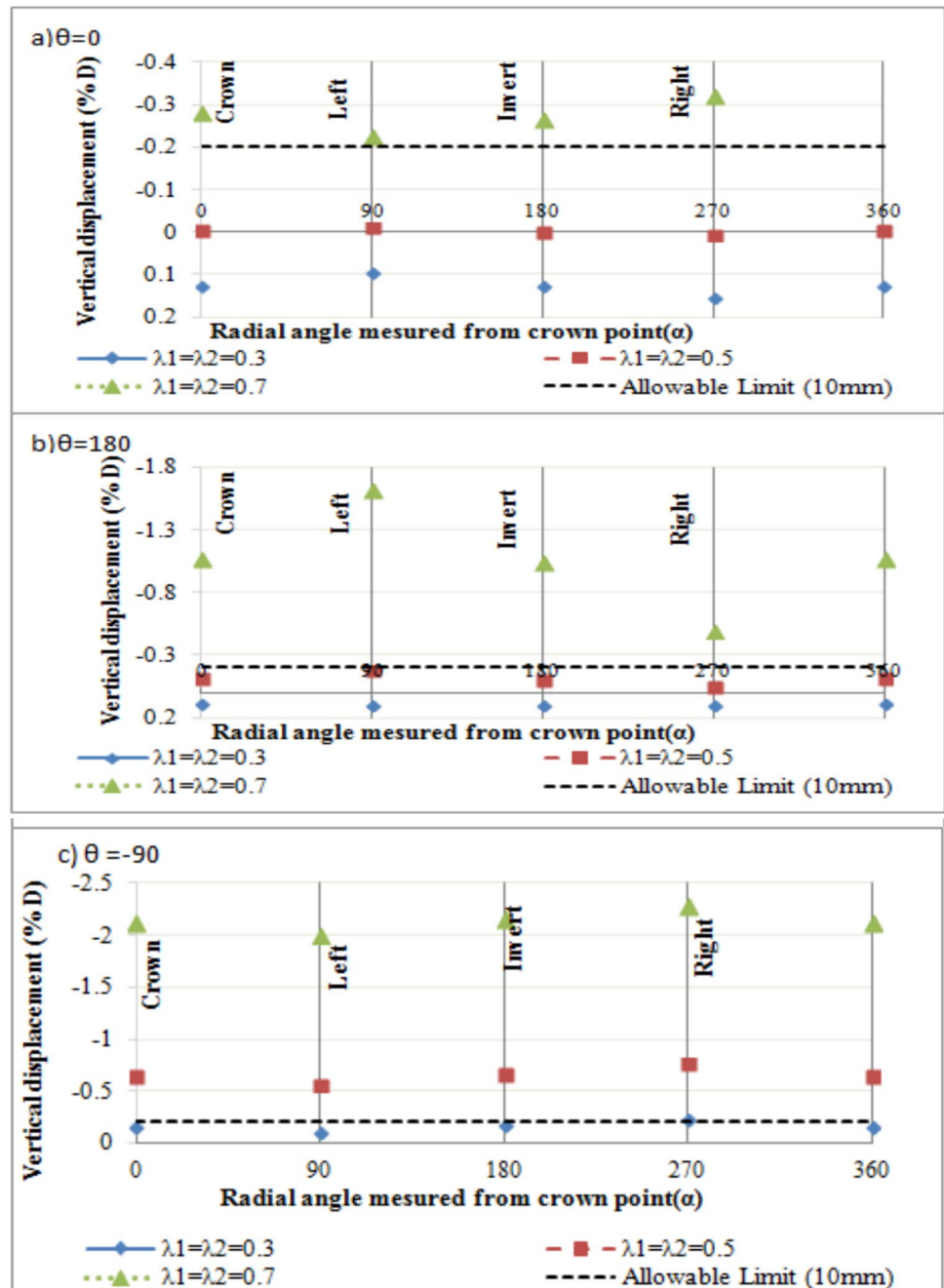
Case 1: In reference case 1, the middle tunnel was excavated first, followed by the right tunnel (labeled MT-RT), and the inverted case 1 (described RT-MT).

Case 2: In reference case 2, the middle tunnel was excavated first, followed by the left one (named MT-LT), and the inverted case 2 (named LT-MT).

Case 3: In reference case 3, the middle tunnel was excavated first, followed by the down one (named MT-DT), and the inverted case 3 (named DT-MT).

The comparison of maximum surface settlements  $S_{max}$ , maximum surface horizontal displacement of the slope  $H_{max}$  and the lining forces between two opposite construction sequences for each relative position achieved in numerical simulations are listed in Table 4. The surface settlement caused by the right tunnel being excavated first (RT-MT) is the greatest. The eventual surface settlement caused by the left tunnel excavated at first (LT-MT) is, on the other hand, the least. As a result, the tunnel excavation sequence of excavating the left tunnel first and subsequently the middle tunnel (LT-MT) is recommended. These results agree with the study of Li et al. (2023) [24]. He revealed that the same excavation sequence is more conducive to ensuring slope stability for twin tunnels aligned horizontally under a loose rock slope. Concerning the horizontal alignment, the construction of the right tunnel at first then the middle (RT-MT) leads to higher settlement and internal forces compared to that obtained by the construction of the middle at first MT-RT. The maximum settlement in the inverted case (RT-MT) is higher by about 48% and sharper than that induced in the reference case MT-RT; while, the bending moment and the axial force of the right tunnel in the first case are higher by about 17.5% and 98%, respectively, than that induced in the second case. The case of (MT-LT) leads to higher settlement and internal forces compared to that obtained by the case of (LT-MT). The maximum settlement in the reference case (MT-LT) is higher by about 44.8% than that in the inverted case LT-MT; while, the bending moment and the axial force of the left tunnel in the first case are higher by about 24% and 30% than that induced in the second case. Concerning the vertical alignment, the case of (DT-MT) leads to smaller soil settlement than that induced in the case of (MT-DT). This result agrees with the study of Hage and Shahrour (2008) [7]. The maximum settlement in the reference case (MT-DT) is higher by about 13.5% than that in the inverted case DT-MT, while little changes in the bending moment of the down tunnel in the two cases. Finally, unlike the tunnel constructed below horizontal ground, where the maximum subsidence is positioned vertically above the tunnel’s centerline and symmetric shape, the results show a shift in maximum subsidence away from the tunnel’s centerline and toward the downward slope. Furthermore, the surface

**Fig. 10** Effect of different values of the stress release coefficient of the second tunnel ( $\lambda_2$ ) at spacing ( $S=1.5D$ ) on the vertical displacement in the first lining ( $m$ ) for different positions of the second tunnel **a** ( $\theta=0$ ), **b** ( $\theta=180$ ) and **c** ( $\theta=-90$ )



inclination and ovalization deformation tunnel cross section result in uplift at the toe zone of the slope and asymmetric shape for the surface settlement pattern.

**The influence of the Slope Angle:**

For a constant soil type (medium sand) and constant spacing ( $S=2D$ ), Fig. 11 illustrates the impact of the slope angle on the slope deformation and the structural forces in the first tunnel (at the middle of the slope) after excavating a new one at different positions. For the shallower slope, the critical

position for the slope deformation induces at  $\theta=-90^\circ$  as mentioned before. As the slope angle increases, the effect of the twin tunnel excavations becomes more profound on the slope deformation and the tunnel’s stability, especially at the position of  $\theta=180^\circ$ . This confirms the fact that excavating a new tunnel close to the base of the steep slope contributes to destabilize the slope more significantly than in another situation (center or head) of the tunnel in the slope (Koizumi et al. 2010) [52].

In the case of a steeper slope ( $\alpha=33.7^\circ$ ) and the position of  $\theta=180^\circ$ , the value of maximum horizontal displacement

**Table 4** Displacement and lining forces results due to the excavation sequences

Reference and inverted cases	Smax(m)	Hmax(m)	Maximum bending moment in the tunnel lining (kN.m/m)		Maximum axial force (kN/m)		Settlement pattern
Case1							
MT-RT	0.0826	0.0445	MT= 139.9	RT= 131	MT=437.44	RT= 374	U shape
RT-MT	0.1226	0.0605	MT= 116.4	RT= 154	MT=337.85	RT= 742	V shape
Case2							
MT-LT	0.0912	0.054	MT= 130.26	LT=82.27	MT=378.8	LT=262.8	V shape
LT-MT	0.063	0.0338	MT= 107.27	LT=102	MT=314.14	LT=343	V shape
Case3							
MT-DT	0.107	0.047	MT= 89.24	DT= 158	MT=303.8	DT=471.9	V shape
DT-MT	0.0942	0.0437	MT= 75.5	DT= 159	MT=260	DT= 506	V shape

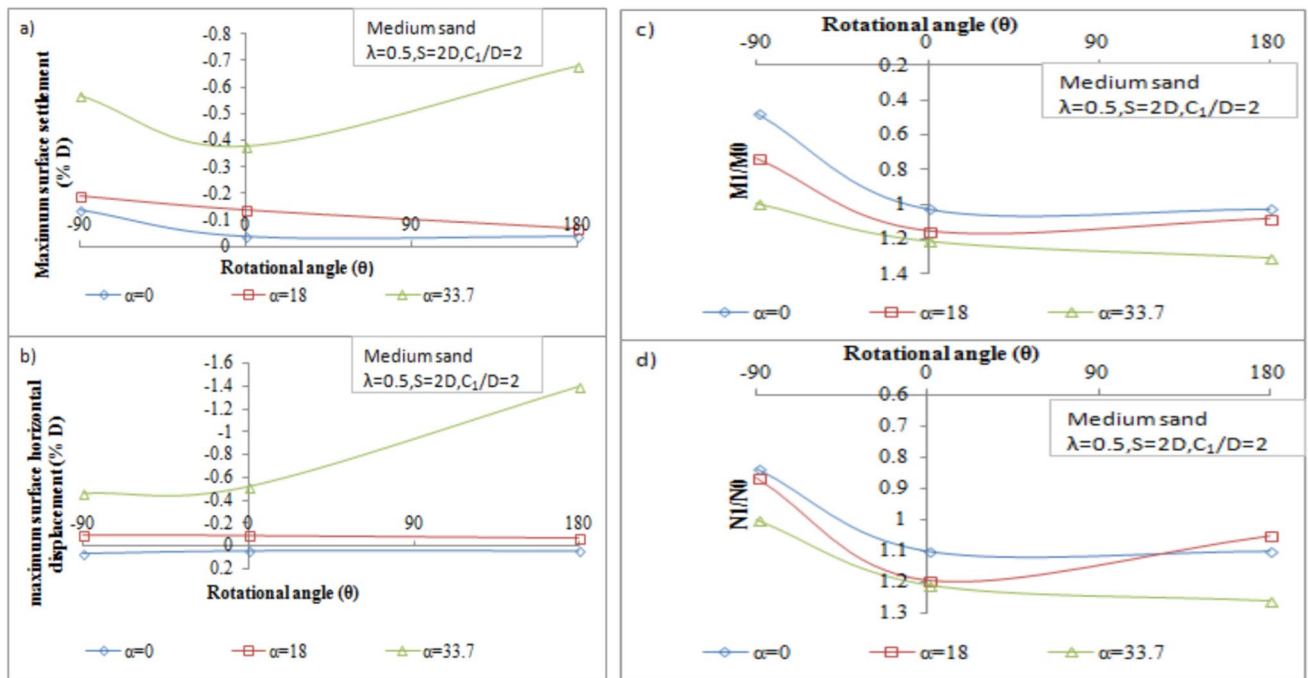


**Fig. 11** Effect of slope angle ( $\alpha$ ) on **a** the surface settlement, **b** the surface horizontal movement, **c** the moment ratio, and **d** the axial force ratio

of the slope is higher than the surface settlement by about 100%. Also, the maximum bending moment and the axial force in the first tunnel are higher by about 30% and 26%, respectively, than that induced in the case of the first tunnel only. Therefore, it can be inferred that as the slope becomes steeper, it is more susceptible to the stability of the slope and the first tunnel. Thus, it is recommended in such cases to avoid excavating the new tunnels toward the toe in steeper slopes.

**Tunnel Depth Effects**

For a constant soil type (medium sand), constant spacing ( $S=2D$ ), and steeper slope ( $\alpha = 33.7^\circ$ ), as shown in Fig. 12, the tunnel depth greatly influences the ground surface

settlement and the horizontal displacement. As the tunnel depth decreases, the settlement and the horizontal displacement of the ground surface increase. When the cover depth of the first tunnel is more than  $2D$  and  $4D$ , the effect of the cover depth on the ground surface settlement and horizontal displacement, respectively, becomes very small. A significant increase will occur in the surface displacement for the cover depth of the first tunnel closer than  $2D$ . The surface horizontal displacement in the slope becomes greater than the surface settlement up to cover depth  $2.5$ . Thus, it is recommended that the supporting structures should be installed in time during the construction of the shallow tunnels in steeper slopes to reduce horizontal movements and avoid slope failure. The moment coefficient and the axial force coefficient of the first tunnel will increase significantly if

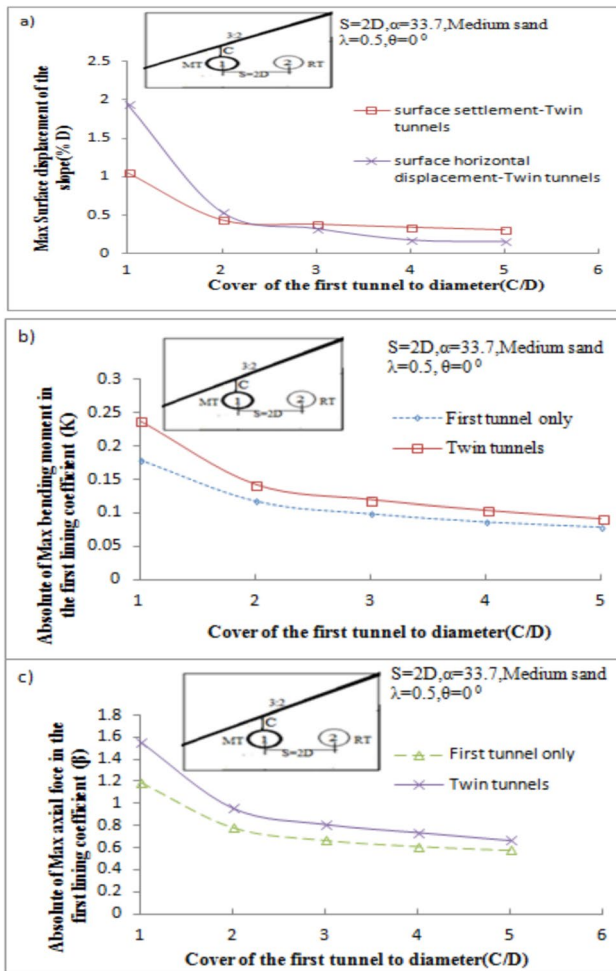


**Fig. 12** Influence of the first tunnel cover depth ( $C_1/D$ ) on **a** the surface settlement and the surface horizontal movement, **b** the moment coefficient, and **c** the axial force coefficient

the first tunnel’s cover depth is less than (2–3) times the tunnel diameter.

**Validation:**

**Numerically:**

A 50% stress release ratio ( $\lambda_d$ ) was employed by the CCM method to model twin tunnels constructed in sand soil and presented by Hage and Shahrour (2008) [7]. Two tunnels aligned horizontally at depth  $H/D = 2.5$  and spacing  $S/D = 2$  were compared to the finding of the presented model for the identical material properties as published by Hage and Shahrour (2008) [7]. The comparison is presented in Fig. 13 for the twin tunnels beneath a horizontal ground surface. In addition, a comparison with a single tunnel in clayey sand soil was performed with the same horizontal ground surface,

material, and geometric conditions as adopted by (Do 2014) [32]. Variable values of stress release ratio ( $\lambda_d$ ) were applied from 0.1 to 0.75. The comparison is presented in Fig. 14. Good agreement was found with both studies.

**Empirically:**

It is possible to predict surface settlement by empirical methods. One of the famous empirical methods is the Herzog method. Herzog (1985) [2] proposed an empirical equation to predict the value of the maximum surface settlement for twin tunnels by Equation (4). The formula is as follows:

$$S_{max} = 4.71(\gamma Z_0 + \sigma_s) \frac{D^2}{(3i+a)E} \quad (4) \text{ Herzog (1985) [2]}$$

Where  $D$  is the tunnel diameter,  $\gamma$  is the unit weight,  $E$  is the elasticity modulus of the soil (kPa),  $\sigma_s$  is the surcharge at the surface,  $a$  is the spacing between the tunnel axes,  $Z_0$  is the tunnel depth (m) and  $i$  is the point of inflection (m). The point of inflection ( $i$ ) can be obtained from Eq. (5), which can be applied to all soil types.

$$i = 0.386Z_0 + 2.84 \quad (5) \text{ Arioglu, (1992) [53]}$$

However, the surface Settlement values obtained in the previous empirical estimations obey some limitations such as circular tunnel shape, the excavation by NATM at shallow depths and the formation is clay soil. Furthermore, the ground surface is horizontal. In this study; the previous empirical equation will be used to estimate the maximum ground settlements and compared with the numerical results in the case of the horizontal ground surface.

A comparison of 2D numerical simulations of tunneling with Herzog method is demonstrated in Fig. 15 for different spacing values between the two tunnels. The results are compared with the present numerical model by Plaxis 2D in the case of horizontal ground by using equation 1. In loose sand, the Herzog technique is effective for estimating the maximum surface settlement values above the twin tunnels. Furthermore, it can predict the effect of twin tunnel spacing on maximum surface settlement.

**Conclusion**

The purpose of this study is to investigate the effect of geometric parameters such as spacing rotation and cover depth, as well as excavation parameters such as the construction sequence and the stress release coefficient, on the changes induced in the slope surface and first tunnel by the excavation of a new one beneath the slope surface.

1 The assumption of considering the value of the stress release ratio=50% for shallow twin tunnels constructed

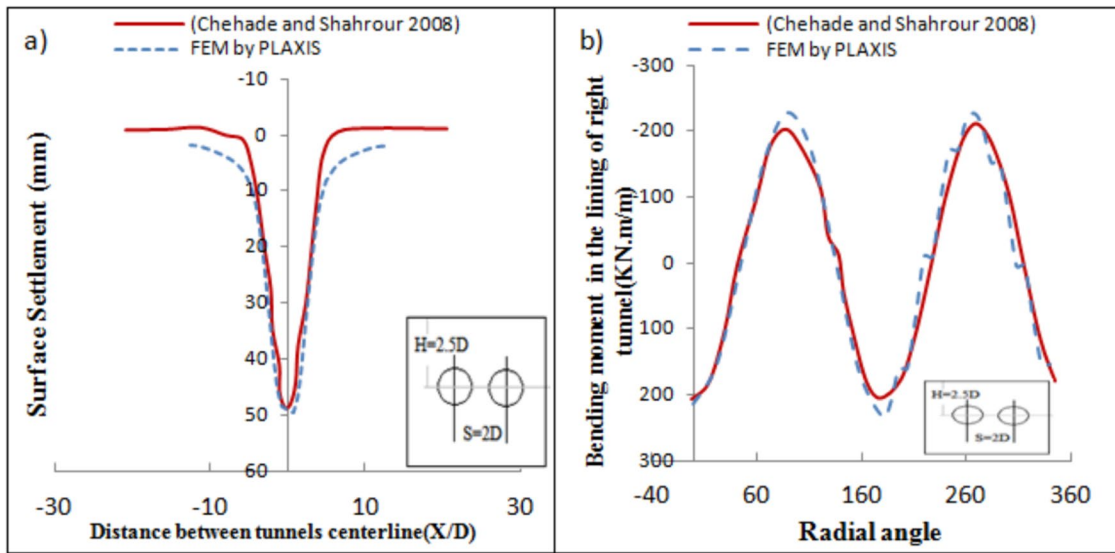


**Fig. 13** Comparison between the presented model and Hage and Shahrour (2008) [7] where **a** ground surface settlement (*mm*); and **b** the bending moment in the new tunnel lining (*kN.m/m*)

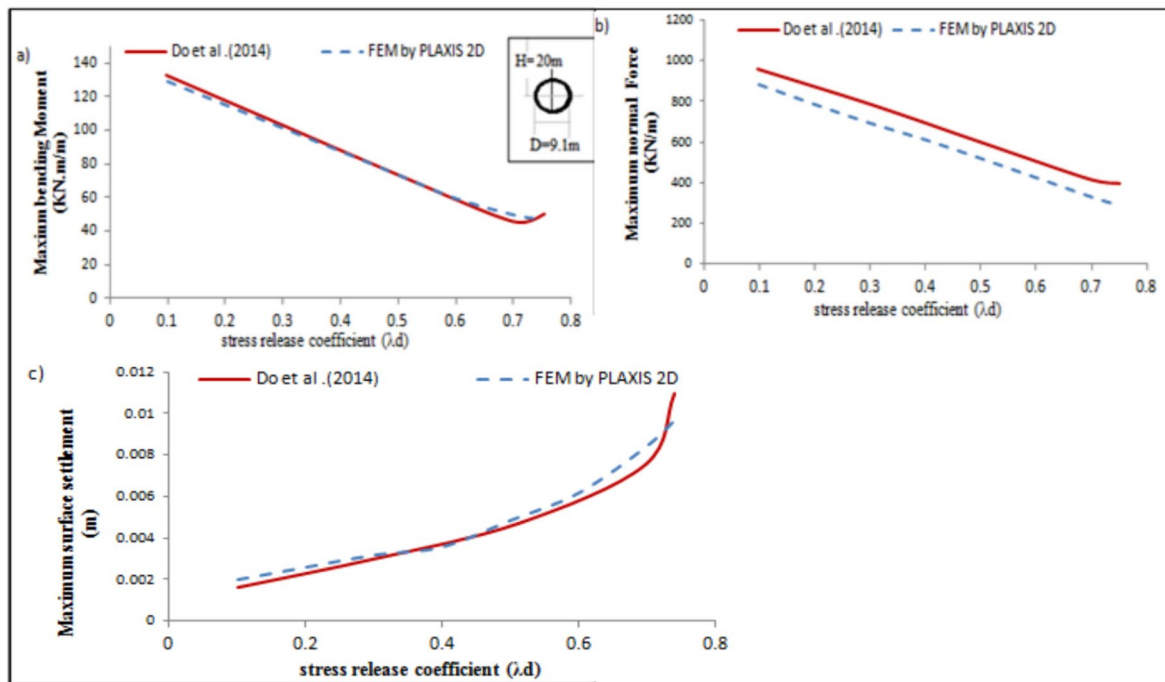


**Fig. 14** Comparison of the present results obtained for the same conditions as reported by (Do 2014) [32] for variable stress release coefficient ( $\lambda_d$ ) with **a** the bending moment in the single tunnel (*kN.m/m*),

**b** the normal force in the single tunnel (*kN/m*) and **c** ground surface settlement(*m*)

in loose sand on a shallow slope (3:1) may result in the following results:

1. Unlike the tunnel constructed below horizontal ground, where the maximum subsidence is positioned vertically above the tunnel's centerline and

symmetric shape, the results show a shift in maximum subsidence away from the tunnel's centerline and toward the downward slope. Furthermore, the surface inclination and ovalization deformation tunnel cross section result in uplift at the toe zone of

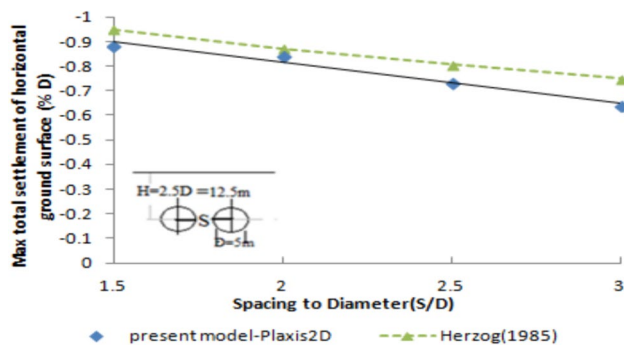


**Fig. 15** Maximum surface settlement values based on empirical and numerical models for twin tunnels in loose sand under horizontal surface

the slope and asymmetric shape for the surface settlement pattern.

- According to the design charts, the displacements in the slope surface caused by the second tunnel may increase or decrease with the variation in spacing values depending on the position of the new tunnel. If the highest horizontal or vertical deformation of the slope surface above the first tunnel is detected, the surface displacements above the second tunnel can be simply estimated from the charts. Changing the spacing  $S$  has little effect on the surface settlement and the straining action in the first tunnel in the case of  $\theta = -90^\circ$  compared to the other position. At the same spacing and cover depth, the position of  $\theta = -90^\circ$  causes the largest deformation in the first tunnel lining and the largest slope surface settlements for all different sand soil types.
- The extent of maximum surface settlement of the slope varied for each of the new tunnel positions. The new tunnel had a large portion of the total settlement located directly above the tunnel at the positions of  $\theta = 180^\circ$  and  $-90^\circ$ ; whereas, the position of  $\theta = 0^\circ$  spreads the maximum settlement over a larger area under the top zone. This position may represent a danger to the buildings and other urban structures.
- The moment coefficient and the axial force coefficient of the first tunnel will increase significantly after excavating the new one at spacing less than (2.5–3) times the tunnel diameter. This outcome is valid for all three positions of the new tunnel.
- The surface settlement caused by the right tunnel being excavated first (RT-MT) is the greatest. The eventual surface settlement caused by the left tunnel excavated first (LT-MT) is, on the other hand, the smallest and most optimal excavation sequence.
- The results differed significantly between loose and medium soils compared to medium and dense sand

soils. Therefore, the loose sandy slopes should be compacted if it is possible before excavating the tunnels. In addition, It is important to reach a certain relative density with compaction, after which compaction does not affect the results.

## 2 Considering the influence of the stress release ratio value

- The proposed charts show how to calculate the critical design values of stress release coefficients for new tunnels without the necessity for relatively expensive slope and first tunnel lining strengthening techniques. These critical design values are related to the tunnel configuration parameters in loose sandy slope and may differ with different soil and tunneling properties.
- At the desired surface settlement, the designer can compare the lining cost of the new tunnel at the proposed design value of  $\lambda_2$  from the chart with the cost of lining and soil strengthening in case of the assumed value of  $\lambda = 0.5$ . Moreover, the value of the stress release coefficient of the second tunnel ( $\lambda_2$ ) is considered a constraint in relative positions and spacing determination. Therefore, the results highlighted the significance of assessing the stress release ratio of the second tunnel ( $\lambda_2$ ).

## 3 The case of shallow twin tunnels constructed in medium sand soil and a steep slope (3:2) may result in the following results:

- In contrast to the tunnels constructed in the shallow slopes, where the surface settlement of the slope is more than the surface horizontal displacement, the surface horizontal displacement in the steep slope becomes greater than the surface settlement up to cover depth  $2.5D$ . Therefore, it is recommended that the supporting structures should be installed in time during the tunneling process in steep slopes.
- The surface displacement, the moment coefficient and the axial force coefficient of the first tunnel will increase significantly after excavating the new one if the first tunnel's cover depth is less than (2–3) times of the tunnel diameter.
- As the slope angle increases, the effect of the twin tunnel excavations at a shallow depth becomes more profound on the slope deformation and the tunnel's stability, especially at the position of  $\theta = 180^\circ$ . This confirms the fact that excavating a new tunnel close to the base of the steep slope contributes to destabilize the slope more significantly than in another situation (center or head) of the tunnel in the slope.



**Acknowledgements** The authors would like to appreciate the anonymous reviewers giving useful suggestions in improving this article.

**Funding** This study and all authors have received no funding.

#### Declarations

**Conflict of interest** The authors declare that they have no known competing financial interests or personal relationships that could have appeared to influence the work reported in this paper.

## References

- Peck, B. B. (1969). Deep excavation and tunnelling in soft ground, State of the art volume. In 7th ICSMFE 4 225–290
- Herzog M (1985) Die Setzungsmulde Über Seicht Liegenden Tunneln. Berlin Bautechnik 11:375–377
- Addenbrooke TI, Potts DM (2001) Twin tunnel interaction: surface and subsurface effects. *Int J Geomech* 1(2):249–271
- Kim CY, Bae GJ, Hong SW, Park CH, Moon HK, Shin HS (2001) Neural network based prediction of ground surface settlements due to tunnelling. *Compt Rendus Geosci* 28(6–7):517–547
- Koungelis D. K and Augarde C. E (2004). Interaction between multiple tunnels in soft ground. In Developments in mechanics of structures and materials. In: Proceedings of the 18th Australian conference on the mechanics of structures and materials]
- Karakus M, Ozsan A, Basarir H (2007) Finite element analysis for the twin metro tunnel constructed in Ankara Clay-Turkey. *Bull Eng Geol Env* 66:71–79
- Hage Chehade F, Shahrour I (2008) Numerical analysis of the interaction between twin-tunnels: Influence of the relative position and construction procedure. *Tunn Undergr Sp Tech* 23:210–214
- Chakeri H, Ozcelik Y, Unver B (2015) Investigation of ground surface settlement in twin tunnels driven with EPBM in urban area. *Arab J Geosci* 8:7655–7666
- Ng CW, Lee KM, Tang DK (2004) Three-dimensional numerical investigations of new Austrian tunnelling method (NATM) twin tunnel interactions. *Can Geotech J* 41(3):523–539
- karademir, S. M. (2010). A parametric study on three dimensional modeling of parallel tunnel interactions (Master's thesis, Middle East Technical University).
- Li, X., Du, S., and Zhang, D. (2013). Numerical simulation of the interaction between two parallel shield tunnels. In: ICPTT 2012 Better Pipeline Infrastructure for a Better Life 1521–1533
- Abdelrehim MZ, Eid MA, Moshref O (2018) Improving the existing roadway tunnels capacity by adding new tunnels—a structural approach. *Arab J Geosci* 11:1–15
- Islam MS, Iskander M (2022) Effect of geometric parameters and construction sequence on ground settlement of offset arrangement twin tunnels. *Geosciences* 12(1):41
- Pedro AM, Grazina JC, Almeida e Sousa JN (2022) Lining forces in tunnel interaction problems. *Soils Rocks* 45(1):12. <https://doi.org/10.28927/SR.2022.077221>
- Du, J. H., and Huang, H. W. (2008). Mechanical behavior of closely spaced tunnels—laboratory model tests and FEM analyses. In: geotechnical aspects of underground construction in soft ground 659–664. CRC Press]
- Lei M, Peng L, Shi C (2015) Model test to investigate the failure mechanisms and lining stress characteristics of shallow buried tunnels under unsymmetrical loading. *Tunn Undergr Space Technol* 46:64–75
- Das R, Singh PK, Kainthola A, Panthee S, Singh TN (2017) Numerical analysis of surface subsidence in asymmetric parallel highway tunnels. *J Rock Mech Geotech Eng* 9(1):170–179
- Vlachopoulos N, Vazaios I, Madjdabadi BM (2018) Investigation into the influence of excavation of twin-bored tunnels within weak rock masses adjacent to slopes. *Can Geotech J* 55(11):1533–1551
- Zhang Q., Wang J., Wang W., Bai S., Lin, P. (2019). Study on slope stability due to the influence of excavation of the high-speed rail tunnel. *Geomatics, Natural Hazards and Risk*.
- Banerjee SK, Chakraborty D (2018) Stability of long circular tunnels in sloping ground. *Geomech Geoeng* 13(2):104–114
- Yang C, Hu Z, Huang D, Guo F (2020) Failure mechanism of primary support for a shallow and asymmetrically loaded tunnel portal and treatment measures. *J Perform Constr Facil* 34(1):4019105
- Song D, Liu X, Chen Z, Chen J, Cai J (2021) Influence of tunnel excavation on the stability of a bedded rock slope: a case study on the mountainous area in southern Anhui, China. *KSCE J Civ Eng* 25:114–123
- Qiu H, Qiu R, Luo G, Ayasrah MM, Wang Z (2022) Study on the mechanical behavior of fluid–solid coupling in shallow buried tunnels under different biased terrain. *Symmetry* 014(7):1339
- Li C, Zheng H, Hu Z, Liu X, Huang Z (2023) Analysis of loose surrounding rock deformation and slope stability at shallow double-track tunnel portal: a case study. *Appl Sci* 13(8):5024
- Dias, T. G. S., and Bezuijen, A. (2014). Tunnel modelling: Stress release and constitutive aspects. In Geotechnical Aspects of Underground Construction in Soft Ground-8th International Symposium (IS-Seoul). CRC Press/Balkema, Leiden, Seoul, South Korea 197–202 DOI:<https://doi.org/10.1201/b17240-37>
- Panet, M. and Guenot, A. (1982), “Analysis of convergence behind the face of a tunnel”, Proceedings of the International Symposium, Tunnelling-82, Brighton, U.K., June.
- Fenner, R. (1938). Untersuchungen zur erkenntnis des gebirgsdrucks. (No Title)]
- Pacher, F. (1964). Deformationsmessungen im Versuchsstollen als Mittel zur Erforschung des Gebirgsverhaltens und zur Bemessung des Ausbaues. In Grundfragen auf dem Gebiete der Geomechanik/Principles in the Field of Geomechanics: XIV. Kolloquium der Österreichischen Regionalgruppe (i. Gr.) der Internationalen Gesellschaft für Felsmechanik/14th Symposium of the Austrian Regional Group (if) of the International Society for Rock Mechanics Salzburg, 27. und 28. September 1963 149–161 Springer Berlin Heidelberg.
- Negro, A., and Eisenstein, Z. (1997). Panel discussion: Delayed lining activation and ground stress relaxation in shallow tunnels. In: Comptes rendus du quatorzième conférence internationale de Mécanique des sols et des travaux de fondation, Hambourg, 6–12 4 2391 CRC Press.]
- Mousivand M, Maleki M, Nekooei M, Mansoori MR (2017) Application of convergence–confinement method in analysis of shallow non-circular tunnels. *Geotech Geol Eng* 35:1185–1198
- Mroueh H, Shahrour I (2008) A simplified 3D model for tunnel construction using tunnel boring machines. *Tunn Undergr Space Technol* 23(1):38–45
- Do, N. A. (2014). Numerical analyses of segmental tunnel lining under static and dynamic loads, Doctoral dissertation, INSA de Lyon.
- Wood AM (1975) The circular tunnel in elastic ground. *Geotechnique* 25(1):115–127
- Kim HJ, Eisenstein Z, Chae BG, Jeong CH (2006) Estimates of stress reduction factors for the tunnel design. *Tunn Undergr Sp Technol inc Trenchless Technol Res* 21(3):451–451
- Svoboda, T., and Mašín, D. (2010). Convergence-confinement method for simulating NATM tunnels evaluated by comparison

- with full 3D simulations. In: Proceedings of the 11th international conference on underground construction, 795–801.
36. Möller SC, Vermeer PA (2008) On numerical simulation of tunnel installation. *Tunn Undergr Space Technol* 23:461–475
  37. Zhang XM, Liu XF, He F (2008) Influence of stress releasing ratio and boundary scope on 2D FEM simulate. *J Coal Sci Eng (China)* 14:604–607
  38. Heidarzadeh H, Kamgar R (2020) Evaluation of the importance of gradually releasing stress around excavation regions in soil media and the effect of liners installation time on tunneling. *Geotech Geol Eng* 38(2):2213–2225
  39. Li, F., Liu, W., Tang, X., and Gan, P. (2014). Numerical research on the influence of stress release on tunnel face stability. In: ICPTT 2014 creating infrastructure for a sustainable world 799–807]
  40. Sun Qiang, Qiang; Dias, Daniel, (2019) Assessment of stress relief during excavation on the seismic tunnel response by the pseudo-static method. *Soil Dyn Earthquake Eng* 117:384–97. <https://doi.org/10.1016/j.soildyn.2018.09.0190>
  41. Nie J, He C, Kou H, Liu F, Yang W (2024) Research on excavation method for soft rock tunnel based on stress release rate. *Appl Sci* 14(2):668
  42. Causse, L., Cojean, R., and Fleurisson, J. A. (2015). Interactions Between Tunnels and Unstable Slopes: Role of Excavation, In: *Engineering Geology for Society and Territory-Volume 2 Landslide Processes*, 237–242, Springer International Publishing]
  43. Brinkgreve RBJ, Vermeer PA (2002) PLAXIS Version 8: Finite element code for soil and rock analyses. AA Balkema, Netherlands
  44. McGrath, T. J., Selig, E. T., Webb, M. C., and Zoladz, G. V. (1999). Pipe interaction with the backfill envelope (No. FHWA-RD-98–191). University of Massachusetts at Amherst. Transportation Center.]
  45. McGrath, T. J. (2002). Recommended specifications for large-span culverts (Vol. 473). Transportation Research Board]
  46. Balkaya M, Moore ID, Sağlamer A (2013) Study of non-uniform bedding support under continuous PVC water distribution pipes. *Tunn Undergr Space Technol* 35:99–108
  47. Zhou, M., Wang, F., and Du, Y. J. (2018). Numerical modeling on localized ground subsidence induced by the tunneling in sand. In: *Proceedings of geoshanghai 2018 international conference tunneling and underground construction* 84–92 Springer Singapore.]
  48. Hefny, A. M., Chua, H. C., and Zhao, J. (2004). Parametric studies on the interaction between existing and new bored tunnels, tunnelling and underground space technology, underground space for suitable urban development. In: *Proceedings of the 30th ITA-AITES world tunnel congress*.
  49. Vinod M, Khabbaz H (2019) Comparison of rectangular and circular bored twin tunnels in weak ground. *Undergr Space* 4(4):328–339
  50. Kim, S. H., and Kim, S. H. (1996). Model testing and analysis of interactions between tunnels in clay (Doctoral dissertation, University of Oxford)]
  51. El-Naiem A, Abdou M, Mohamed A-W, W. (2007) Behavior of existing tunnel due to the construction of a new tunnel passed parallel under it. *JES J Eng Sci* 35(6):1381–1400
  52. Koizumi, Y., Lee, J., Date, K., Yokota, Y., Yamamoto, T., and Fujisawa, K. (2010, June). Numerical analysis of landslide behavior induced by tunnel excavation. In *ISRM EUROCK* (pp. ISRM-EUROCK). ISRM
  53. Arioglu E (1992) Surface movements due to tunnelling activities in urban areas and minimization of building damages. Short Course, Istanbul Technical University, Mining Engineering Department ((in Turkish))

**Publisher’s Note** Springer Nature remains neutral with regard to jurisdictional claims in published maps and institutional affiliations.

Springer Nature or its licensor (e.g. a society or other partner) holds exclusive rights to this article under a publishing agreement with the author(s) or other rightsholder(s); author self-archiving of the accepted manuscript version of this article is solely governed by the terms of such publishing agreement and applicable law.